

A High-Pressure Study of the Effects of TiO₂ Nanoparticles on the Structural Organization of Ionic Liquids

Hai-Chou Chang,^{*,†} Shu-Chieh Chang,[†] Tzu-Chieh Hung,[†] Jyh-Chiang Jiang,[‡] Jer-Lai Kuo,[§] and Sheng Hsien Lin^{§,⊥}

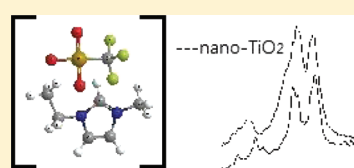
[†]Department of Chemistry, National Dong Hwa University, Shoufeng, Hualien 974, Taiwan

[‡]Department of Chemical Engineering, National Taiwan University of Science and Technology, Taipei 106, Taiwan

[§]Institute of Atomic and Molecular Sciences, Academia Sinica, P.O. Box 23-166, Taipei 106, Taiwan

[⊥]Department of Applied Chemistry, National Chiao Tung University, Hsinchu 30010, Taiwan

ABSTRACT: The local structures between nano-TiO₂ and 1-ethyl-3-methylimidazolium trifluoromethanesulfonate (EMI⁺TFS⁻) and 1-butyl-3-methylimidazolium trifluoromethanesulfonate (BMI⁺TFS⁻) were investigated using high-pressure infrared spectroscopy. No significant changes in C–H spectral features of EMI⁺TFS⁻ were observed in the presence of nano-TiO₂ under ambient pressure. As the EMI⁺TFS⁻/nano-TiO₂ mixture was compressed to 0.3 GPa, the imidazolium C–H absorptions became two sharp bands at 3108 and 3168 cm⁻¹, respectively, and the alkyl C–H stretching absorption exhibits a new band at 3010 cm⁻¹ associated with a weaker band at 3028 cm⁻¹. It appears that pressure stabilizes the isolated conformations due to pressure-enhanced imidazolium C–H—nano-TiO₂ interactions. Our results also reveal that alkyl C–H groups play non-negligible roles at the conditions of high pressures. The results of BMI⁺TFS⁻/nano-TiO₂ are remarkably different from what is revealed for EMI⁺TFS⁻/nano-TiO₂. The spectral features and band frequencies of BMI⁺TFS⁻/nano-TiO₂ are almost identical to those of pure BMI⁺TFS⁻ under various pressures. This study demonstrates that changes to the alkyl chain length of the cation could be made to control the order and strength of ionic liquid/nano-TiO₂ interactions.



INTRODUCTION

Ionic liquids have received widespread interest as a promising alternative to conventional volatile organic solvents.^{1–4} In systems using ionic liquids as solvents, the decrease in vapor pressure can be explained by the negligible vapor pressure of ionic liquids. In the past most of the interest in ionic liquids is centered on the design of new nonvolatile solvents.¹ Although the literature contains a number of articles on the application of ionic liquids as solvents, studies on the phase behavior of ionic liquids in the presence of nanoparticles are scarce in the past. Recently, the self-assembly of ionic liquids and the local structures of ionic liquids in ionic liquid/nanoparticle mixtures have been studied.^{5–9} The ordering of ionic liquids at solid surfaces is a subject of intense research in the recent,^{10–13} while some fundamental questions still remain to be answered regarding the nature of the microscopic states. The properties of interfacial ionic liquids in ionic liquid/nanoparticle mixtures are very complex and unusual that have been shown using experimental and theoretical methods. These properties depend strongly on the structure of surfaces, temperature, and pressure.^{5–13} Generally, the microscopic structures of ionic liquid/nanoparticle mixtures are not fully understood.^{5–13} The purpose of this contribution is to use various pressures as a window to look into the hydrogen-bonding networks of ionic liquid/nano-TiO₂ mixtures.

Among various metal oxides, titanium dioxide has received considerable attention due to its unique physicochemical

properties and chemical stability.^{7,13–15} Nano-sized titanium dioxide, because of the combination of its high surface areas and semiconducting properties, is a promising candidate for a vast range of applications including photovoltaics and energy storage.^{7,13–15} In the dye-sensitized solar cells the dyes are absorbed on a nano-TiO₂ network, and the light absorption of the dyes is followed by an electron injection into the conduction band of the nano-TiO₂ network. Traditionally, the dye-sensitized solar cells are immersed in organic solvents such as acetonitrile. The application of conventional solvents in the dye-sensitized solar cells suffers the problems of evaporation and flammability under warm temperature. The utility of ionic liquids for dye-sensitized solar cells has been reported, avoiding evaporation of conventional solvents. In other words, the system of ionic liquid/nano-TiO₂ may have the potential to be an important component in light-to-electric energy devices.^{7,13,14}

The ionic liquid cation is typically an organic structure of low symmetry to prevent ions from packing easily. The recent research has focused on ionic liquids composed of asymmetric 1-alkyl-3-methylimidazolium cations associated with a variety of anions.^{1–4} 1-Butyl-3-methyl and 1-ethyl-3-methylimidazolium cations are probably the most investigated structures of this class, and they hold three imidazolium C–H bonds constituting

Received: September 1, 2011

Revised: October 25, 2011

Published: October 28, 2011

spectroscopic probes for cation–anion interactions. Whether the imidazolium C–H bonds is involved in directional hydrogen bonding with the anions or solvents is still an issue of debate.^{4,16} Several studies have been performed to elucidate the role of weak hydrogen bonds, such as C–H...O and C–H...X, in the structures of ionic liquids.^{1–4} The C–H covalent bond tends to shorten as a result of formation of a weak hydrogen bond. Associated with this contraction is a shift of the C–H stretching frequency to the blue, as compared to the usual expectation of a red shift. Scheiner's group^{17,18} and Dannenberg's group¹⁹ view conventional and C–H...O hydrogen bonds to be very similar in nature. The origin of both the red- and blue-shifted hydrogen bonds was also concluded to be the same by Schlegel's group²⁰ and Hermansson's group.²¹

An interesting aspect of ionic liquids is that the cations possess an inherent amphiphilicity. Both experiments and theoretical studies display structural heterogeneity in ionic liquids.^{22–25} Aggregation can lead to ordered local environment, even for alkyl chains as short as butyl.²⁵ Among the experimental methods that probe the structures of ionic liquid mixtures, vibrational spectroscopy has its own specific contribution especially on the local organization of C–H groups. Two or three resolved absorption bands are observed with 1-alkyl-3-methylimidazolium salts in the IR spectral region between 3000 and 3200 cm^{−1}. These can be attributed to coupled imidazolium C–H stretching vibrations. Many of the researches are interested in the interactions between anion and water/organic solvent in ionic liquid mixtures.^{1–4} However, some researchers infer the non-negligible role of cation–solvent interactions.^{26,27} Perturbation of hydrogen-bond structures caused by cation–nanoparticle interactions was also reported in the literature.^{9,28}

It is well-known that hydrogen-bonded structures can be distorted by high pressure.^{9,26–32} One can apply high pressure to tune the strength of the hydrogen bond and to destabilize hydrophobic contacts. The various degrees of solvation at high pressure may arise from a reorganization of the hydrogen bond network and/or geometry.^{26–30} Pressure is a fundamental physical property that influences the values of different thermodynamic and kinetic parameters.^{33–35} Pressure-dependence studies reveal information on the volume profile of the process. Pressure affects chemical equilibrium, and the chemical reactions will adjust to favor the components with smaller volume upon compression.^{33–35} Static pressures up to several megabars can be generated using diamond anvil cells. Nevertheless, the pressures used to investigate chemical systems typically range from ambient to several GPa. Such pressure mainly change intermolecular distances and affect conformation.

EXPERIMENTAL SECTION

Samples were prepared using 1-ethyl-3-methylimidazolium trifluoromethanesulfonate (>98%, Fluka), 1-butyl-3-methylimidazolium trifluoromethanesulfonate (>95%, Fluka), and titanium(IV) oxide nanopowder (anatase, 99.7%, Aldrich). A diamond anvil cell (DAC) of Merrill–Bassett design, having a diamond culet size of 0.6 mm, was used for generating pressures up to ca. 2 GPa. Two type IIa diamonds were used for mid-infrared measurements. The sample was contained in a 0.3 mm diameter hole in a 0.25 mm thick inconel gasket mounted on the diamond anvil cell. To reduce the absorbance of the samples, CaF₂ crystals (prepared from a CaF₂ optical window) were placed into the hole and compressed firmly prior to inserting the

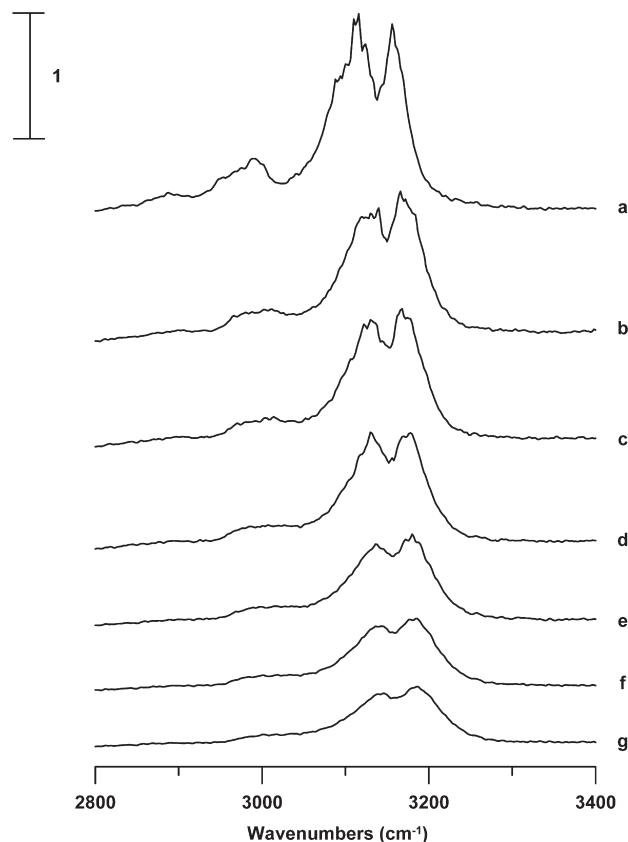


Figure 1. IR spectra of pure EMI⁺TFS[−] obtained under ambient pressure (curve a) and at 0.3 (curve b), 0.9 (curve c), 1.5 (curve d), 1.9 (curve e), 2.3 (curve f), and 2.5 GPa (curve g).

sample. A droplet of a sample filled the empty space of the entire hole of the gasket in the DAC, which was subsequently sealed when the opposed anvils were pushed toward one another. Infrared spectra of the samples were measured on a Perkin-Elmer Fourier transform spectrophotometer (model Spectrum RXI) equipped with a LITA (lithium tantalite) mid-infrared detector. The infrared beam was condensed through a 5X beam condenser onto the sample in the diamond anvil cell. Typically, we chose a resolution of 4 cm^{−1} (data point resolution of 2 cm^{−1}). For each spectrum, typically 1000 scans were compiled. To remove the absorption of the diamond anvils, the absorption spectra of DAC were measured first and subtracted from those of the samples. Pressure calibration follows Wong's method.^{36,37} The pressure dependence of screw moving distances was measured.

RESULTS AND DISCUSSION

We have concentrated our analysis on the 2800–3300 cm^{−1} region which contains the alkyl C–H and imidazolium C–H stretching modes. The trifluoromethanesulfonate anion (CF₃SO₃[−]) is called TFS[−] in this article. Figure 1 displays infrared spectra of pure 1-ethyl-3-methylimidazolium trifluoromethanesulfonate (EMI⁺TFS[−]) obtained under ambient pressure (curve a) and at 0.3 (curve b), 0.9 (curve c), 1.5 (curve d), 1.9 (curve e), 2.3 (curve f), and 2.5 GPa (curve g). The spectrum in Figure 1a shows the alkyl C–H bands locating at 2891, 2953, 2980, and 2991 cm^{−1}, respectively. As indicated in Figure 1a, the imidazolium C–H stretching absorptions separate into two major peaks

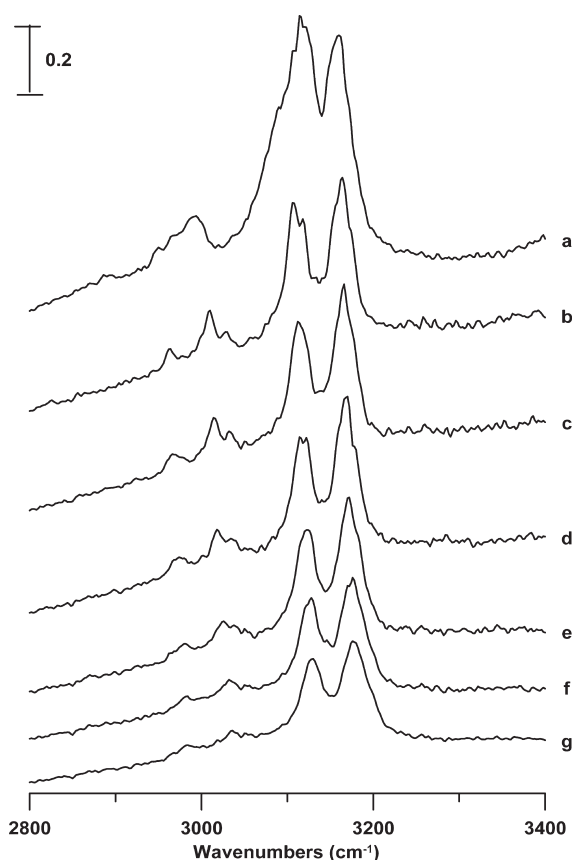


Figure 2. IR spectra of an EMI⁺TFS[−]/nano-TiO₂ mixture (16 wt % nano-TiO₂) obtained under ambient pressure (curve a) and at 0.3 (curve b), 0.9 (curve c), 1.5 (curve d), 1.9 (curve e), 2.3 (curve f), and 2.5 GPa (curve g).

at 3113 and 3157 cm^{−1} associated with one minor shoulder at 3093 cm^{−1}. It is known that the imidazolium C–H stretching region may be described by two doublets (four bands): one doublet at lower frequencies is assigned to the C²–H stretching modes, and another doublet at the higher frequencies is attributed to the coupled C⁴–H and C⁵–H stretching modes.³⁸ The imidazolium C–H may exist in two different forms, i.e., isolated and associated structures, based on previous studies, and the 3093 and 3113 cm^{−1} peaks should be attributed to isolated and associated species, respectively.^{26–30,38} The isolated form means smaller ion clusters (or free ions), and the associated form may be larger ion cluster (or ion pairs). As pure EMI⁺TFS[−] was compressed to the pressure of 0.3 GPa, the two major imidazolium C–H bands were blue-shifted to 3129 and 3170 cm^{−1}, respectively, in Figure 1b. As clearly shown in Figure 1, the imidazolium C–H bands of pure EMI⁺TFS[−] display anomalous nonmonotonic pressure-induced frequency shifts. The imidazolium C–H peaks yield blue frequency shift at pressure below 0.3 GPa (Figure 1a,b), then undergo almost no changes (Figure 1b–d), and then blue-shift again upon increasing the pressure (Figure 1d–g). This discontinuity in frequency shift in Figure 1 is similar to the trend revealed in previous studies of pure 1-ethyl-3-methylimidazolium bis(trifluoromethylsulfonyl)amide (EMI⁺TFSA[−])²⁷ and 1-butyl-3-methylimidazolium hexafluorophosphate (BMI⁺PF₆[−]).³⁹ A possible explanation for this behavior is that both pressure-induced phase transitions and local C–H structural organizations may occur in Figure 1. Analyzing the pressure dependence

of the alkyl C–H stretches yields bandwidth broadening and slightly blue frequency shifts.

Figure 2 shows IR spectra of an EMI⁺TFS[−]/nano-TiO₂ mixture having nano-TiO₂ equal to 16 wt % obtained under ambient pressure (curve a) and at 0.3 (curve b), 0.9 (curve c), 1.5 (curve d), 1.9 (curve e), 2.3 (curve f), and 2.5 GPa (curve g). Looking into more detail in Figures 2a and 1a, we observe no appreciable changes of C–H spectral features in the presence of nano-TiO₂ under ambient pressure in Figure 2a. As the sample was compressed to 0.3 GPa in Figure 2b, the imidazolium C–H stretching modes underwent dramatic changes in their spectral profiles with bandwidth narrowing. The imidazolium C–H absorptions became two sharp bands at 3108 and 3163 cm^{−1} in Figure 2b. The sharper structures reveals in Figure 2b may be caused by the loss in intensity of the bands attributed to the associated structures. In other words, the compression leads to pressure-induced perturbation of isolated–associated equilibrium. It appears that pressure somehow stabilizes the isolated conformation as shown in Figure 2. The pressure-enhanced imidazolium C–H...O interactions between EMI⁺TFS[−] and nano-TiO₂ may be one of the reasons for the transformation from associated structures to isolated species in Figure 2. The similarity in spectral features of Figure 2b–g suggests that the isolated form is stable under the conditions of high pressures up to the pressure of 2.5 GPa. As revealed in Figure 2b, the alkyl C–H stretching absorption exhibits a new sharp band at 3010 cm^{−1} associated with a weaker band at 3028 cm^{−1}. These two new bands, being related to nano-TiO₂ and pressure dependence, may arise from the local structure changes of alkyl C–H groups caused by the pressure-enhanced interactions between ionic clusters and nano-TiO₂. In the past, most of the works on ionic liquid/solid interface paid the attention to the contributions from imidazolium C–H groups under ambient pressure.^{7–13} However, this study demonstrates that alkyl C–H groups^{9,40} play non-negligible roles in ionic liquid/nano-TiO₂ mixtures at the conditions of high pressures.

The surface of titanium dioxide is usually covered with a certain amount of titanol (Ti–OH) groups.⁷ In order to learn the insight of isolated–associated equilibrium, pressure-dependent studies of ionic liquid/H₂O mixtures may provide further evidence. Figure 3 shows IR spectra of an EMI⁺TFS[−]/H₂O mixture having its mole fraction of H₂O equal to 0.3 obtained under ambient pressure (curve a) and at 0.3 (curve b), 0.9 (curve c), 1.5 (curve d), 1.9 (curve e), 2.3 (curve f), and 2.5 GPa (curve g). As shown in Figure 3a, there are no significant changes in the spectral shapes of the C–H stretching bands due to the presence of water molecules in Figure 3a under ambient pressure. As the mixture was compressed to 0.3 GPa, the imidazolium C–H bands were blue-shifted to 3125 and 3165 cm^{−1} in Figure 3b. As the pressure was further elevated to 0.9 GPa, changes in the relative band intensities of isolated/associated imidazolium C–H bands occurred in Figure 3c. As shown in Figure 3c, the compression leads to the decrease in the associated C–H band intensity in the imidazolium C–H absorption region. It is instructive to note that we do not observe experimental evidence of the appearance of the new alkyl C–H features at ca. 3010 and 3028 cm^{−1} in Figure 3c–g. On the basis of the results in Figure 3, we found that the oxygen atoms of H₂O may not significantly perturb the local structures of alkyl C–H groups of EMI⁺TFS[−]. This observation indicates that imidazolium C–H groups are more favorable sites for C–H...OH₂ hydrogen bonding than alkyl C–H groups in the EMI⁺TFS[−]/H₂O mixture.

Figure 4 illustrates the pressure-dependent variations in the band frequencies of imidazolium C–H vibrations. As revealed, we do not observe remarkable differences in the imidazolium

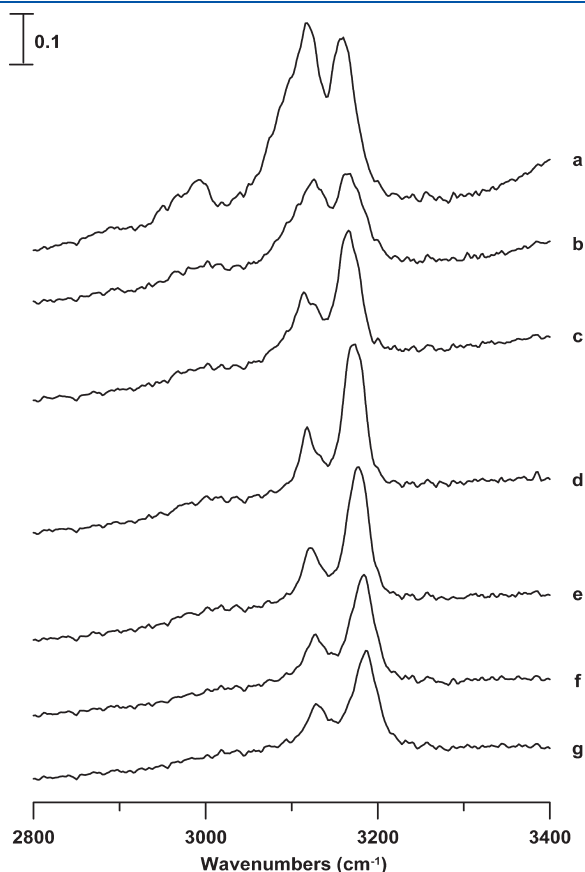


Figure 3. IR spectra of an EMI⁺TFS[−]/H₂O mixture having its mole fraction of H₂O equal to 0.3 obtained under ambient pressure (curve a) and at 0.3 (curve b), 0.9 (curve c), 1.5 (curve d), 1.9 (curve e), 2.3 (curve f), and 2.5 GPa (curve g).

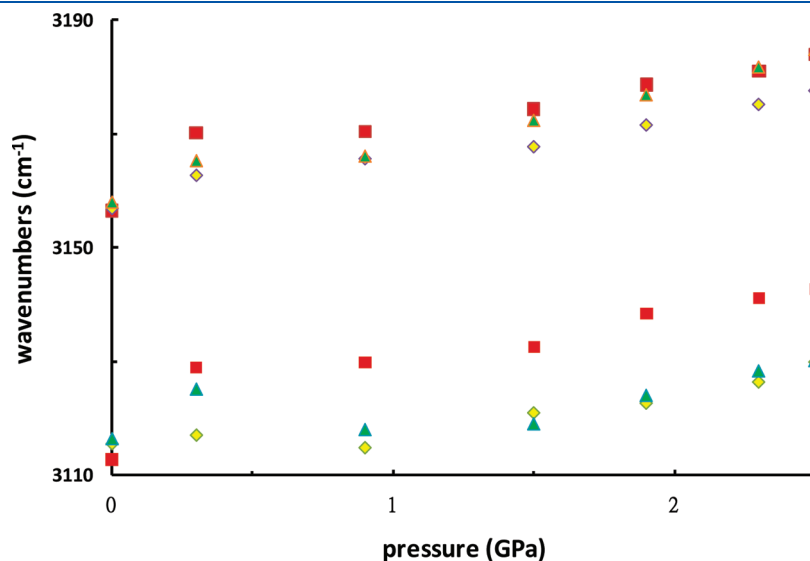


Figure 4. Pressure dependence of the imidazolium C–H stretching frequencies of pure EMI⁺TFS[−] (squares), the EMI⁺TFS[−]/nano-TiO₂ mixture (diamonds), and the EMI⁺TFS[−]/H₂O mixture (triangles).

C–H band frequencies for pure EMI⁺TFS[−], EMI⁺TFS[−]/nano-TiO₂, and EMI⁺TFS[−]/H₂O, respectively, at ambient pressure in Figure 4. The coupled imidazolium C–H band at ca. 3113 cm^{−1} displays a red shift under the pressure of 0.9 GPa as nano-TiO₂ or H₂O was added. In other words, both nano-TiO₂ and H₂O can change network configurations at C²–H local regions as the pressure is elevated. In contrast to the band at ca. 3113 cm^{−1}, the addition of H₂O does not induce red shifts in frequency for the imidazolium C–H band at ca. 3157 cm^{−1} under high pressures ($p > 1$ GPa). The band positions (at ca. 3157 cm^{−1}) of pure EMI⁺TFS[−] and EMI⁺TFS[−]/H₂O remain approximately the same as the pressure was increased up to 2.5 GPa. This observation can be physically related to the well-known acidity of imidazolium C²–H.^{1–4} In the ionic liquid-rich mixtures, the water molecules may prefer to interact with C²–H instead of C⁴–H/C⁵–H to form C–H...O hydrogen bonds. However, the red frequency shift of the imidazolium C–H band at ca. 3157 cm^{−1} is obvious for the EMI⁺TFS[−]/nano-TiO₂ mixture in comparison to pure EMI⁺TFS[−] and EMI⁺TFS[−]/H₂O in Figure 4. As pointed out by Ludwig's group,³⁸ the imidazolium C–H band at ca. 3157 cm^{−1} is attributed to the coupled C⁴–H and C⁵–H stretching modes. On the basis of the results shown in Figure 4, nano-TiO₂ can be added to perturb the local structures of C⁴–H and C⁵–H under the conditions of high pressures.

Figure 5 displays infrared spectra of pure 1-butyl-3-methylimidazolium trifluoromethanesulfonate (BMI⁺TFS[−]) obtained under ambient pressure (curve a) and at 0.3 (curve b), 0.9 (curve c), 1.5 (curve d), 1.9 (curve e), 2.3 (curve f), and 2.5 GPa (curve g). As indicated in Figure 5a, the infrared spectrum of pure EMI⁺TFS[−] exhibits three alkyl C–H bands at 2877, 2940, and 2967 cm^{−1}, respectively, and two imidazolium C–H bands at 3116 and 3155 cm^{−1} associated with a shoulder at 3098 cm^{−1}. The alkyl C–H stretches were blue-shifted to 2889, 2958, and 2991 cm^{−1} in Figure 5b. A phase transition, i.e., pressure-induced solidification, was observed, as the imidazolium C–H stretching bands became three separated bands at 3103, 3124, and 3159 cm^{−1} in Figure 5b. Further increases in pressure lead to blue frequency shifts of all C–H stretching bands in Figure 5c–g.

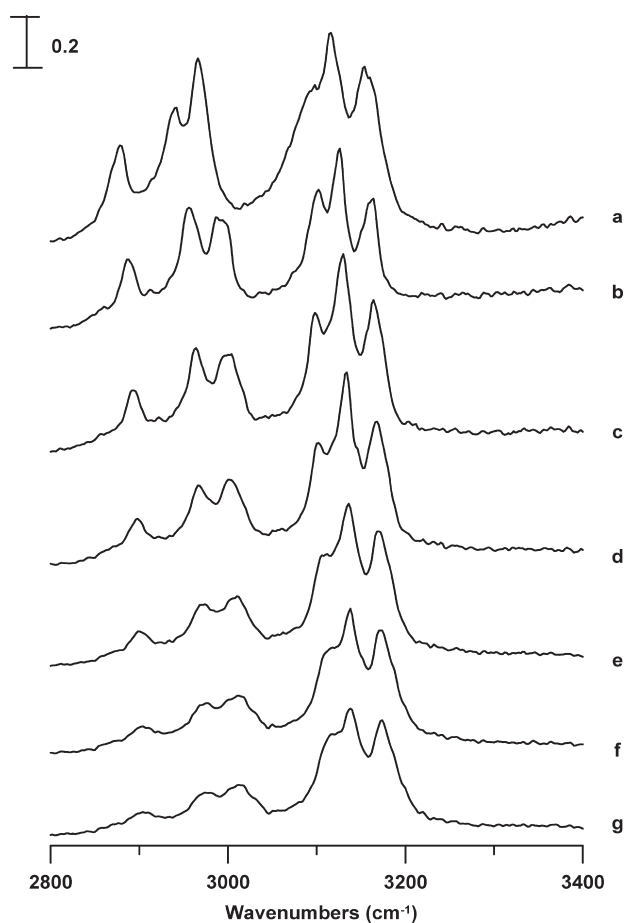


Figure 5. IR spectra of pure BMI⁺TFS[−] obtained under ambient pressure (curve a) and at 0.3 (curve b), 0.9 (curve c), 1.5 (curve d), 1.9 (curve e), 2.3 (curve f), and 2.5 GPa (curve g).

Figure 6 shows IR spectra of a BMI⁺TFS[−]/nano-TiO₂ mixture having 21 wt % nano-TiO₂ obtained under ambient pressure (curve a) and at 0.3 (curve b), 0.9 (curve c), 1.5 (curve d), 1.9 (curve e), 2.3 (curve f), and 2.5 GPa (curve g). As shown in Figures 5 and 6, no appreciable changes in band frequencies and spectral features of C–H vibrations occurred as BMI⁺TFS[−] was mixed with nano-TiO₂ in Figure 6. This result is remarkably different from what is revealed for the EMI⁺TFS[−]/nano-TiO₂ mixture in Figure 2. Figure 7 illustrates the pressure dependence of the band frequency of the two dominant imidazolium C–H stretching absorptions at ca. 3116 and 3155 cm^{−1}. As shown in Figure 7, the band frequencies of the BMI⁺TFS[−]/nano-TiO₂ mixture are almost identical to those of pure BMI⁺TFS[−]. Our results in Figures 5–7 indicate that the presence of nano-TiO₂ does not perturb the ionic liquid–ionic liquid associations of BMI⁺TFS[−] in the imidazolium region. After comparison with the EMI⁺TFS[−]/nano-TiO₂ system, it appears that the increase in alkyl chain length seems to reduce the effects of C–H...nano-TiO₂ interactions under high pressures. In this study we demonstrate that changes to the alkyl chain length of the cation could be made to control the order and strength of ionic liquid/nano-TiO₂ interactions. Both experiments and simulations have found that the alkyl side-chain length has an influence on the supramolecular assemblies of ionic liquids. It was known that sequentially increasing the alkyl chain length leads to an increase in the size of nonpolar domains.^{22–25,41} A minimum of three carbons is

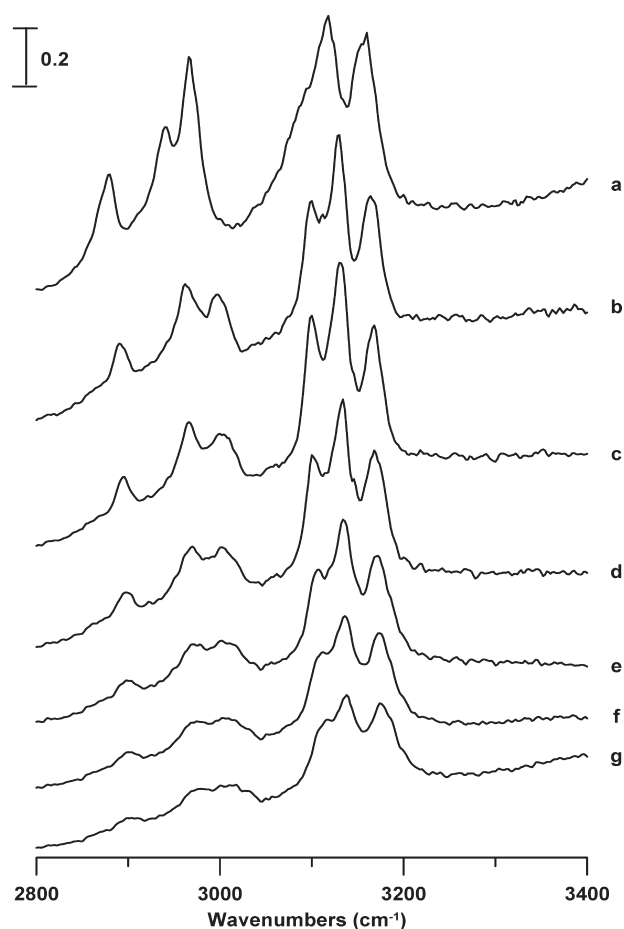


Figure 6. IR spectra of a BMI⁺TFS[−]/nano-TiO₂ mixture (21 wt % nano-TiO₂) obtained under ambient pressure (curve a) and at 0.3 (curve b), 0.9 (curve c), 1.5 (curve d), 1.9 (curve e), 2.3 (curve f), and 2.5 GPa (curve g).

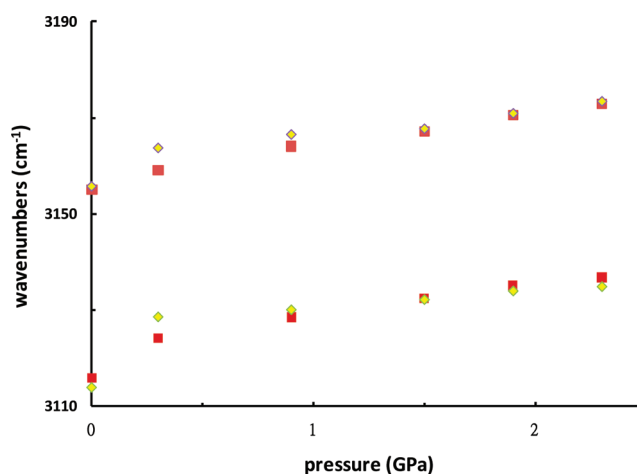


Figure 7. Pressure dependence of the imidazolium C–H stretching frequencies of pure BMI⁺TFS[−] (squares) and a BMI⁺TFS[−]/nano-TiO₂ mixture with 21 wt % nano-TiO₂ (diamonds).

required in the alkyl substituent of the imidazolium cation for the ionic liquids to self-assemble to provide an intermediate range order of nanostructures.²⁵ The results of the present study

indicate that imidazolium C–H nano-TiO₂ interaction may not be the sole factor to reorganize the local structures of ionic liquid/nano-TiO₂ mixtures, while the alkyl C–H groups may also play non-negligible roles in isolated-associated equilibrium.

CONCLUSION

The isolated-associated equilibrium was probed by high-pressure infrared spectroscopy for pure EMI⁺TFS[−], EMI⁺TFS[−]/nano-TiO₂, EMI⁺TFS[−]/H₂O, pure BMI⁺TFS[−], and BMI⁺TFS[−]/nano-TiO₂. Clear effects from the addition of nano-TiO₂ were observed, while it appeared that high pressures stabilize the isolated configurations for the EMI⁺TFS[−]/nano-TiO₂ system. In the presence of nano-TiO₂, the local structures of alkyl C–H, imidazolium C²–H, and imidazolium C^{4,5}–H were perturbed in the EMI⁺TFS[−]/nano-TiO₂ mixture under high pressures. In the ionic liquid-rich EMI⁺TFS[−]/H₂O mixture, the water molecules may prefer to interact with C²–H instead of C^{4,5}–H and alkyl C–H groups. No observable differences in IR features were found between pure BMI⁺TFS[−] and BMI⁺TFS[−]/nano-TiO₂ based on the pressure-dependent results. The alkyl chain-length dependent study indicates that the alkyl C–H groups may play a compensatory role in isolated–associated equilibrium.

AUTHOR INFORMATION

Corresponding Author

*E-mail: hcchang@mail.ndhu.edu.tw. Fax: +886-3-8633570. Phone: +886-3-8633585.

ACKNOWLEDGMENT

The authors thank the National Dong Hwa University and the National Science Council (Contract NSC 98-2113-M-259-005-MY3) of Taiwan for financial support. The authors thank Tsung-Ting Tsai, Leo Yuxiu Li, and Wei-Wen Hung for their assistance.

REFERENCES

- (1) Wasserscheid, P.; Welton, T., Eds.; *Ionic Liquids in Synthesis*; Wiley-VCH: Weinheim, Germany, 2008.
- (2) Castner, E. W.; Wishart, J. F. *J. Chem. Phys.* **2010**, *132*, 120901.
- (3) Weingartner, H. *Angew. Chem., Int. Ed.* **2008**, *47*, 654.
- (4) Wulf, A.; Fumino, K.; Ludwig, R. *Angew. Chem., Int. Ed.* **2010**, *49*, 449.
- (5) Ueno, K.; Hata, K.; Katakabe, T.; Kondoh, M.; Watanabe, M. *J. Phys. Chem. B* **2008**, *112*, 9013.
- (6) Sobota, M.; Schmid, M.; Happel, M.; Amende, M.; Maier, F.; Steinruck, H. P.; Paape, N.; Wasserscheid, P.; Laurin, M.; Gottfried, J. M.; Libuda, J. *Phys. Chem. Chem. Phys.* **2010**, *12*, 10610.
- (7) Aliaga, C.; Baldelli, S. *J. Phys. Chem. C* **2008**, *112*, 3064.
- (8) Liu, Y.; Wu, G.; Fu, H.; Jiang, Z.; Chen, S.; Sha, M. *Dalton Trans.* **2010**, *39*, 3190.
- (9) Chang, H. C.; Hung, T. C.; Chang, S. C.; Jiang, J. C.; Lin, S. H. *J. Phys. Chem. C* **2011**, *115*, 11962.
- (10) Atkin, R.; Abedin, S. Z. E.; Hayes, R.; Gasparotto, L. H. S.; Borisenko, N.; Endres, F. *J. Phys. Chem. C* **2009**, *113*, 13266.
- (11) Hayes, R.; Abedin, S. Z. E.; Atkin, R. *J. Phys. Chem. B* **2009**, *113*, 7049.
- (12) Zhang, J.; Zhang, Q.; Li, X.; Liu, S.; Ma, Y.; Shi, F.; Deng, Y. *Phys. Chem. Chem. Phys.* **2010**, *12*, 1971.
- (13) Wang, S.; Cao, Z.; Li, S.; Yan, T. *Sci. China, Ser. B: Chem.* **2009**, *52*, 1434.

- (14) Hahlin, M.; Johansson, E. M. J.; Scholin, R.; Siegbahn, H.; Rensmo, H. *J. Phys. Chem. C* **2011**, *115*, 11996.
- (15) Fabregat-Santiago, F.; Randriamahazaka, H.; Zaban, A.; Garcia-Canadas, J.; Garcia-Belmonte, G.; Bisquert, J. *Phys. Chem. Chem. Phys.* **2006**, *8*, 1827.
- (16) Grondin, J.; Lassegues, J. C.; Cavagnat, D.; Buffeteau, T.; Johansson, P.; Holomb, R. *J. Raman Spectrosc.* **2011**, *42*, 733.
- (17) Scheiner, S.; Kar, T.; Pattanayak, J. *J. Am. Chem. Soc.* **2002**, *124*, 13257.
- (18) Gu, Y. L.; Kar, T.; Scheiner, S. *J. Am. Chem. Soc.* **1999**, *121*, 9411.
- (19) Turi, L.; Dannenberg, J. J. *J. Phys. Chem.* **1993**, *97*, 7899.
- (20) Li, X.; Liu, L.; Schlegel, H. B. *J. Am. Chem. Soc.* **2002**, *124*, 9639.
- (21) Hermansson, K. *J. Phys. Chem. A* **2002**, *106*, 4695.
- (22) Schroder, U.; Wadhawan, J. D.; Compton, R. G.; Marken, F.; Suarez, P. A. Z.; Consorti, C. S.; de Souza, R. F.; Dupont, J. *New J. Chem.* **2000**, *24*, 1009.
- (23) Lopes, J. N. A. C.; Padua, A. A. H. *J. Phys. Chem. B* **2006**, *110*, 3330.
- (24) Wang, Y.; Voth, G. A. *J. Phys. Chem. B* **2006**, *110*, 18601.
- (25) Xiao, D.; Hines, L. G.; Li, S.; Bartsch, R. A.; Quitevis, E. L.; Russina, O.; Triolo, A. *J. Phys. Chem. B* **2009**, *113*, 6426.
- (26) Jiang, J. C.; Lin, K. H.; Li, S. C.; Shih, P. M.; Hung, K. C.; Lin, S. H.; Chang, H. C. *J. Chem. Phys.* **2011**, *134*, 044506.
- (27) Jiang, J. C.; Li, S. C.; Shih, P. M.; Hung, T. C.; Chang, S. C.; Lin, S. H.; Chang, H. C. *J. Phys. Chem. B* **2011**, *115*, 883.
- (28) Chang, H. C.; Jiang, J. C.; Tsai, W. C.; Chen, G. C.; Lin, S. H. *Chem. Phys. Lett.* **2006**, *427*, 310.
- (29) Umabayashi, Y.; Jiang, J. C.; Shan, Y. L.; Lin, K. H.; Fujii, K.; Seki, S.; Ishiguro, S.; Lin, S. H.; Chang, H. C. *J. Chem. Phys.* **2009**, *130*, 124503.
- (30) Umabayashi, Y.; Jiang, J. C.; Lin, K. H.; Shan, Y. L.; Fujii, K.; Seki, S.; Ishiguro, S.; Lin, S. H.; Chang, H. C. *J. Chem. Phys.* **2009**, *131*, 234502.
- (31) Jablonski, M.; Sadlej, A. J. *Chem. Phys. Lett.* **2008**, *463*, 322.
- (32) Russina, O.; Fazio, B.; Schmidt, C.; Triolo, A. *Phys. Chem. Chem. Phys.* **2011**, *13*, 12067.
- (33) Asano, T.; le Noble, W. J. *Chem. Rev.* **1978**, *78*, 407.
- (34) Van Eldik, R.; Asano, T.; le Noble, W. J. *Chem. Rev.* **1989**, *89*, 549.
- (35) Drljaca, A.; Hubbard, C. D.; van Eldik, R.; Asano, T.; Basilevsky, M. V.; le Noble, W. J. *Chem. Rev.* **1998**, *98*, 2167.
- (36) Wong, P. T. T.; Moffatt, D. J.; Baudais, F. L. *Appl. Spectrosc.* **1985**, *39*, 733.
- (37) Wong, P. T. T.; Moffatt, D. J. *Appl. Spectrosc.* **1987**, *41*, 1070.
- (38) Koddermann, T.; Wertz, C.; Heintz, A.; Ludwig, R. *ChemPhysChem* **2006**, *7*, 1944.
- (39) Chang, H. C.; Jiang, J. C.; Tsai, W. C.; Chen, G. C.; Lin, S. H. *J. Phys. Chem. B* **2006**, *110*, 3302.
- (40) Takekiyo, T.; Imai, Y.; Hatano, N.; Abe, H.; Yoshimura, Y. *Chem. Phys. Lett.* **2011**, *511*, 241.
- (41) Greaves, T. L.; Kennedy, D. F.; Kirby, N.; Drummond, C. J. *Phys. Chem. Chem. Phys.* **2011**, *13*, 13501.